

# Overview of the SuperNova/Acceleration Probe (SNAP)

G. Aldering<sup>a</sup>, C. Akerlof<sup>b</sup>, R. Amanullah<sup>c</sup>, P. Astier<sup>d</sup>, E. Barrelet<sup>d</sup>, C. Bebek<sup>a</sup>, L. Bergström<sup>c</sup>, J. Bercovitz<sup>a</sup>, G. Bernstein<sup>e</sup>, M. Bester<sup>f</sup>, A. Bonissent<sup>g</sup>, C. Bower<sup>h</sup>, W. Carithers<sup>a</sup>, E. Commins<sup>f</sup>, C. Day<sup>a</sup>, S. Deustua<sup>i</sup>, R. DiGennaro<sup>a</sup>, A. Ealet<sup>g</sup>, R. Ellis<sup>j</sup>, M. Eriksson<sup>c</sup>, A. Fruchter<sup>k</sup>, J-F. Genat<sup>d</sup>, G. Goldhaber<sup>f</sup>, A. Goobar<sup>c</sup>, D. Groom<sup>a</sup>, S. Harris<sup>f</sup>, P. Harvey<sup>f</sup>, H. Heetderks<sup>f</sup>, S. Holland<sup>a</sup>, D. Huterer<sup>l</sup>, A. Karcher<sup>a</sup>, A. Kim<sup>a</sup>, W. Kolbe<sup>a</sup>, B. Krieger<sup>a</sup>, R. Lafever<sup>a</sup>, J. Lamoureux<sup>f</sup>, M. Lampton<sup>f</sup>, M. Levi<sup>a</sup>, D. Levin<sup>b</sup>, E. Linder<sup>a</sup>, S. Loken<sup>a</sup>, R. Malina<sup>m</sup>, R. Massey<sup>n</sup>, T. McKay<sup>b</sup>, S. McKee<sup>b</sup>, E. Mörtzell<sup>c</sup>, N. Mostek<sup>h</sup>, S. Mufson<sup>h</sup>, J. Musser<sup>h</sup>, P. Nugent<sup>a</sup>, H. Oluseyi<sup>a</sup>, R. Pain<sup>d</sup>, D. Pankow<sup>f</sup>, S. Perlmutter<sup>a</sup>, R. Pratt<sup>f</sup>, E. Prieto<sup>m</sup>, A. Refregier<sup>n</sup>, J. Rhodes<sup>o</sup>, K. Robinson<sup>a</sup>, N. Roe<sup>a</sup>, M. Sholl<sup>f</sup>, M. Schubnell<sup>b</sup>, G. Smadja<sup>p</sup>, G. Smoot<sup>f</sup>, A. Spadafora<sup>a</sup>, G. Tarle<sup>b</sup>, A. Tomasch<sup>b</sup>, D. Vincent<sup>d</sup> and J. Walder<sup>a</sup>

<sup>a</sup>Lawrence Berkeley National Laboratory, Berkeley CA, USA

<sup>b</sup>University of Michigan, Ann Arbor MI, USA

<sup>c</sup>University of Stockholm, Stockholm, Sweden

<sup>d</sup>CNRS/IN2P3/LPNHE, Paris, France

<sup>e</sup>University of Pennsylvania, Philadelphia PA, USA

<sup>f</sup>University of California, Berkeley CA, USA

<sup>g</sup>CNRS/IN2P3/CPPM, Marseille, France

<sup>h</sup>Indiana University, Bloomington IN, USA

<sup>i</sup>American Astronomical Society, Washington DC, USA

<sup>j</sup>California Institute of Technology, Pasadena CA, USA

<sup>k</sup>Space Telescope Science Institute, Baltimore MD, USA

<sup>l</sup>Case Western Reserve University, Cleveland OH, USA

<sup>m</sup>CNRS/INSU/LAM, Marseille, France

<sup>n</sup>Cambridge University, Cambridge, UK

<sup>o</sup>Goddard Space Flight Center, Greenbelt MD, USA

<sup>p</sup>CNRS/IN2P3/IPNL, Lyon, France

## ABSTRACT

The SuperNova / Acceleration Probe (SNAP) is an experiment designed to address fundamental questions concerning the cosmological model of our universe and the nature of its constituents. It is centered around a 2-m space telescope, a wide-field imager comprised of CCD and HgCdTe devices, and a low-resolution spectrograph. Cross-cutting and complementary measurement approaches will be used to improve the systematic, as well as statistical, uncertainties. The baseline mission will obtain high signal-to-noise photometric and spectroscopic observations of roughly 2800 Type Ia supernovae out to redshift 1.7 and use those supernovae as “calibrated standard candles.” A wide-field gravitational weak lensing survey, Type II supernovae expanding photosphere distance and strong lensing also will be major components of the cosmology program. The mission design is primarily driven by the requirements for the next generation of these experiments, after the planned ground-based work of the next five years has reached its limits. To advance these cosmological measurements to levels of precision equaling those of the complementary cosmic microwave background satellite work of MAP and PLANK, it will be necessary to control or eliminate the sources of systematic uncertainty much more completely than will be possible with other planned facilities. SNAP is targeted at a level of systematic uncertainties that

will make it possible to begin to discriminate between theories of the “dark energy” that apparently is accelerating the expansion of the universe. We will discuss the latest developments in this design phase of the project.

**Keywords:** Early universe—instrumentation: detectors—space vehicles: instruments—supernovae:general—telescopes

## 1. INTRODUCTION

In the past decade the study of cosmology has taken its first major steps as a precise empirical science, combining concepts and tools from astrophysics and particle physics. The most recent of these results have already brought surprises. The Universe’s expansion is apparently accelerating rather than decelerating as expected solely due to gravity. This implies that the simplest model for the Universe – flat and dominated by matter – appears not to be true, and that our current fundamental physics understanding of particles, forces, and fields is likely to be incomplete.

The clearest evidence for this surprising conclusion comes from the recent supernova measurements of changes in the Universe’s expansion rate that directly show the acceleration. Figure 1 shows the results of Ref. 1 (see also Ref. 2) who use a Hubble diagram for 42 SNe with  $0.18 < z < 0.83$  to find that for a flat universe  $\Omega_M = 0.28 \pm 0.08$  ( $\Omega_\Lambda = 1 - \Omega_M$ ), or a deceleration parameter  $q_0 = -0.58$ , and constrain the combination  $0.8 \Omega_M - 0.6 \Omega_\Lambda$  to  $-0.2 \pm 0.1$ .

This evidence for a negative-pressure vacuum energy density is in remarkable concordance with combined galaxy cluster measurements,<sup>3</sup> which are sensitive to  $\Omega_M$ , and current CMB results,<sup>4,5</sup> which are sensitive to the curvature  $\Omega_k$  (see Fig. 1). Two of these three independent measurements and standard inflation would have to be in error to make the cosmological constant (or other negative pressure dark energy) unnecessary in the cosmological models.

These measurements indicate the presence of a new, unknown energy component that can cause acceleration, hence having equation of state  $w \equiv p/\rho < -1/3$ . This might be the cosmological constant. Alternatively, it could be that this dark energy is due to some other primordial field for which  $\rho \neq -p$ , leading to different dynamical properties than a cosmological constant. The fundamental importance of a universal vacuum energy has sparked a flurry of activity in theoretical physics with several classes of models being proposed (e.g. “quintessence”,<sup>6,7</sup> Pseudo-Nambu-Goldstone Boson (PNGB) models,<sup>8,9</sup> cosmic defects<sup>10,11</sup>). Placing some constraints on possible dark energy models, Refs. 1 and 12 find that for a flat Universe, the data are consistent with a cosmological-constant equation of state with  $0.2 \lesssim \Omega_M \lesssim 0.4$  (Fig. 2), or generally  $w < -0.4$  at 95% confidence level. The cosmic string defect theory ( $w = -1/3$ ) is already strongly disfavored.

In this paper, we attempt to formulate a definitive supernova study that will determine the values of the cosmological parameters and measure the properties and test possible models for the dark energy. In §2 we identify and demonstrate how to minimize systematic errors that fundamentally limit the precision with which this probe can measure cosmological parameters. A supernova dataset that maximizes the resolving power of the redshift-luminosity relation under the constraint of these systematic errors is constructed in §3. We present in §4 the Supernova / Acceleration Probe (SNAP) (Fig. 3) whose observing strategy and instrumentation suite is tailored to provide the data that satisfy both our statistical and systematic requirements.

## 2. CONTROL OF SYSTEMATIC UNCERTAINTIES

Type Ia supernovae have already proven to be an excellent distance indicator for probing the dynamics of the universe. However, as we move toward the era of precision cosmology, we recognize that using the supernova redshift-luminosity distance relationship for measuring cosmological parameters is fundamentally limited by potential systematic errors. Below are identified possible systematic errors any experiment that wishes to make maximal use of this technique will need to recognize and limit.

*Malmquist Bias:* A flux-limited sample preferentially detects intrinsically brighter objects. Attempts to correct this bias rely on knowledge of the SN Ia luminosity function which may change with lookback time. A detection threshold fainter than peak by at least five times the intrinsic SN Ia luminosity dispersion will comfortably ensure a complete sample of unextincted supernovae at our target redshifts and allow detection of previously unobserved very subluminal supernovae.

*K-Correction and Cross-Filter Calibration:* The current data set of time and stretch dependent SN spectra is incomplete. Judicious choice of filter sets, spectral time series of representative SN Ia, and cross-wavelength relative flux calibration will provide  $< 0.01$  errors.

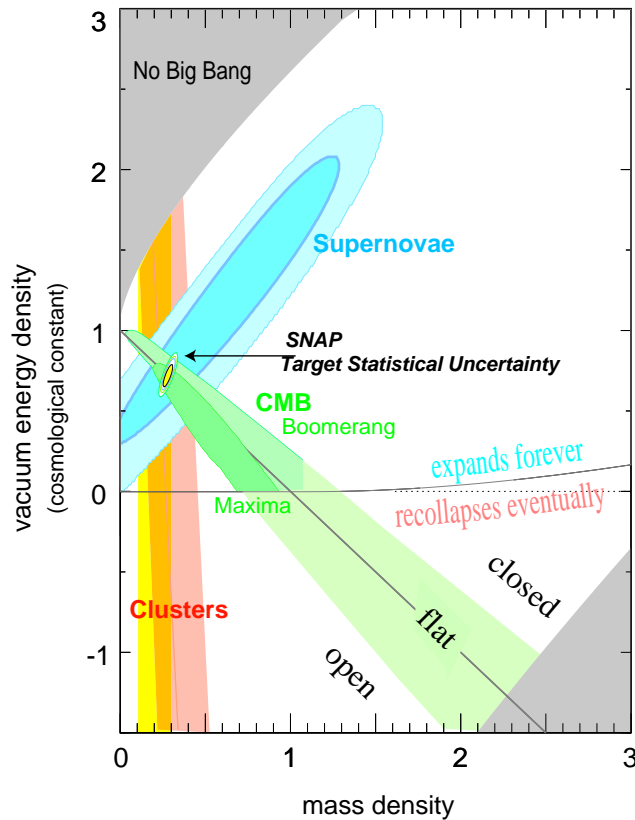


**Figure 1.** There is strong evidence for the existence of a cosmological vacuum energy density. Plotted are  $\Omega_M$ — $\Omega_\Lambda$  confidence regions for current SN,<sup>1</sup> galaxy cluster, and CMB results. These results rule out a simple flat, [ $\Omega_M = 1, \Omega_\Lambda = 0$ ] cosmology. Their consistent overlap is a strong indicator for dark energy. Also shown is the expected confidence region from the SNAP satellite for an  $\Omega_M = 0.28$  flat Universe.

*Non-SN Ia Contamination:* Observed supernovae must be positively identified as SN Ia. As some Type Ib and Ic supernovae have spectra that otherwise mimic those of SNeIa, a spectrum covering the defining rest frame Si II 6250Å feature for every supernova at maximum will provide a pure sample.

*Milky Way Galaxy Extinction:* Supernova fields can be chosen toward the low extinction Galactic poles. SDSS and SIRTf observations, as well as spectra of Galactic subdwarfs, will provide precise Galactic extinction measurements in the direction of supernova (1%).

*Gravitational Lensing by Clumped Mass* Inhomogeneities along the supernova line of sight can gravitationally magnify or demagnify the supernova flux. Large statistics per redshift bin can average out the increased brightness dispersion induced by this effect. Weak gravitational lensing measurements of target fields can provide independent measures of expected de/magnification (2%).

*Extinction by Extra-Galactic “normal” Dust:* Cross-wavelength flux calibrated spectra will measure any wavelength dependent absorption (1%).

*Extinction by Gray Dust:* As opposed to normal dust, gray dust is postulated to produce wavelength independent absorption in optical bands. However, even gray dust cannot remain completely invisible, since it will re-emit absorbed light from galaxies and QSO’s and contribute to the far-infrared background. Deeper SCUBA and SIRTf observations should tighten the constraints on the amount of gray dust allowed.

Dark Energy  
Unknown Component,  $\Omega_{D.E.}$ , of Energy Density  
Supernova Cosmology Project  
Perlmutter et al. (1999)

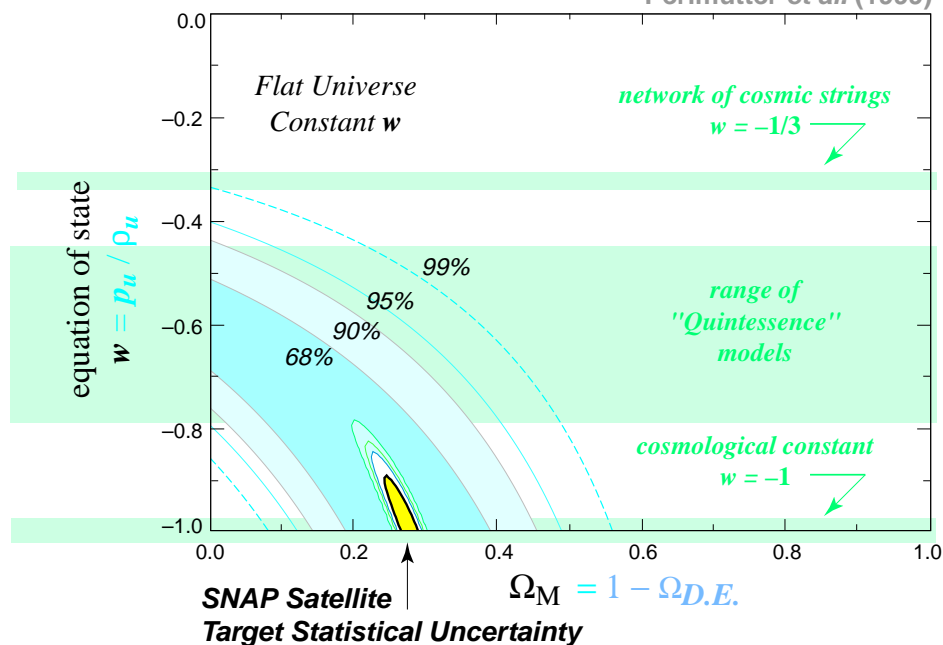


**Figure 2.** Best-fit 68%, 90%, 95%, and 99% confidence regions in the  $\Omega_M - w$  plane for an additional energy density component,  $\Omega_w$ , characterized by an equation-of-state  $w = p/\rho$ . (For Einstein’s cosmological constant,  $\Lambda$ ,  $w = -1$ .) The fit is constrained to a flat cosmology ( $\Omega_M + \Omega_w = 1$ ). Also shown is the expected confidence region allowed by SNAP assuming  $w = -1$  and  $\Omega_M = 0.28$ .

Although physical gray dust grain models dim blue and red optical light equally, the near-IR light ( $\sim 1.2 \mu\text{m}$ ) is less affected. Cross-wavelength calibrated spectra extending to wavelength regions where “gray” dust is no longer gray will characterize the hypothetical large-grain dust’s absorption properties. Armed with the extinction – color excess properties of the gray dust, broadband near-infrared colors can provide “gray” dust extinction corrections for supernovae out to  $z = 0.5$  at controlled SN-explosion epochs.

It should also be noted that reasonable distributions of gray dust will not mimic  $\Omega_M - \Omega_\Lambda$  cosmology Hubble diagrams. For example,  $\{\Lambda = 0, \text{gray dust}\}$  models and  $\{\Lambda \neq 0, \text{no gray dust}\}$  models which are both consistent with current supernova data are expected to diverge at higher redshifts, to the 50 standard-deviation level at redshifts beyond  $z = 1.4$  (2%).

### Uncorrected Evolution

Supernova behavior may depend on properties of its progenitor star or binary-star system. The distribution of these stellar properties is likely to change over time—“evolve”—in a given galaxy, and over a set of galaxies. Nearby SNe Ia drawn from a wide range of galactic environments provide an observed<sup>13, 14</sup> and correctable evolutionary range of SNe Ia. So far, it appears that the differences that have been identified are well calibrated by the SN Ia light curve width-luminosity relation. It is not clear that any additional, more subtle effects that may exist would change the peak luminosity of the SNe Ia.

Our philosophy in bounding possible supernova evolution is as follows. Single-parameter corrections have reduced the dispersion in peak  $B$  supernova brightnesses down to 10% in current data. There is strong evidence that two parameters can further reduce that dispersion. As of yet, there is no evidence for systematic residuals at the 2% level after correction, although observational errors would obscure such an effect. We expect that upcoming low-redshift supernova surveys will expose further heterogeneity of Type Ia supernovae and perhaps even improve our calibrated candle. Theoretical models can identify observables that are expected to display heterogeneity. But the state of empirical understanding of these observables at the time SNAP flies will be explicitly tested by SNAP measurements.

In particular, we demand sensitivity to the effects of evolution on the peak brightness to 2%, to match the uncertainties due to the other systematic errors. These key features, indicative of the underlying physics of the supernova, are:

*Rise time from explosion to peak:* The rise time to peak is an indicator of opacity, fused  $^{56}\text{Ni}$  mass and possible differences in the  $^{56}\text{Ni}$  distribution. Ref. 15 find that a 0.3 days uncertainty corresponds to a 3% brightness constraint at peak. This accuracy requires discovery within  $\sim 2$  days of explosion, on average, i.e.  $\sim 30\times$  fainter than peak.

*Plateau level 45 days past peak:* The light curve plateau level that begins  $\sim 45$  days past peak is an important indicator of the C/O ratio of the progenitor star, and fused  $^{56}\text{Ni}$ . A 10% constraint on this plateau brightness corresponds to a 2% constraint on the peak brightness.<sup>15</sup> This accuracy requires a signal-to-noise ratio of 10 for photometry  $13\times$  fainter than peak.

*Overall light curve timescale:* The “stretch factor” that parameterizes the linear stretching or compression of the light curve time scale is affected by almost all the aforementioned parameters since it tracks the SN Ia’s evolution from early to late times. It is closely correlated with the two previously mentioned observables, which focus on details of the light curve timescale, and it ties this experiment’s controls for systematics to the controls used in the previous ground-based work. A 1.5% uncertainty in the stretch factor measurement corresponds to a  $\sim 2\%$  uncertainty at peak.<sup>1</sup>

*Spectral line velocities:* The velocities of several spectral features throughout the UV and optical make an excellent diagnostic of the overall kinetic energy of the SNe Ia. The kinetic energy directly influences the overall shape of the light curve. If the velocities are constrained to  $\sim 500 \text{ km s}^{-1}$  then the peak luminosity can be constrained to  $\sim 2\%$  uncertainty at peak,<sup>15</sup> given a typical SNe Ia expansion velocity of  $15,000 \text{ km s}^{-1}$ .

*Spectral Feature Ratios:* The ratios of various spectral features in the restframe UV are strong indicators of the metallicity of the SNe Ia. By achieving a reasonable signal-to-noise per wavelength bin we will be able to constrain the metallicity of the progenitor to 0.1 dex (cf. Ref. 16).

We also note that the ratios of spectral features in the restframe optical (Ca II H&K and Si II at  $6150 \text{ \AA}$ ) provide additional constraints on the opacity and luminosity of the SN Ia.<sup>17</sup> These features are easily observed given the velocity measurements mentioned above. By measuring all of these features for each supernova we can tightly constrain the physical conditions of the explosion, making it possible to recognize sets of supernovae with matching initial conditions. The current theoretical models of SN Ia explosions are not sufficiently complete to predict the precise luminosity of each supernova, but they are able to give the rough relationships between changes in the physical conditions of the supernovae (such as opacity, metallicity, fused nickel mass, and nickel distribution) and changes in their peak luminosities. We can therefore give the approximate accuracy needed for the measurement of each feature to ensure that the physical condition of each set of supernovae is well enough determined so that the range of luminosities for those supernovae is well below the systematic uncertainty bound ( $\sim 2\%$  in total).

In addition to these features of the supernovae themselves, we will also study the host galaxy of the supernova. We can measure the host galaxy luminosity, colors, morphology, type, and the location of the supernova within the galaxy, even at redshifts  $z \sim 1.7$ . These observations are not possible from the ground.

### 3. SUPERNOVAE AS A PROBE OF THE DARK ENERGY

Our primary scientific objective is to use most efficiently the leverage available in the redshift-luminosity distance relationship to measure the matter and dark energy densities of the universe with small statistical and systematic errors, and also test the properties and possible models for the dark energy. We thus determine the number of supernovae we need to find, how they should be distributed in redshift, and how precisely we need to determine each one’s peak brightness.

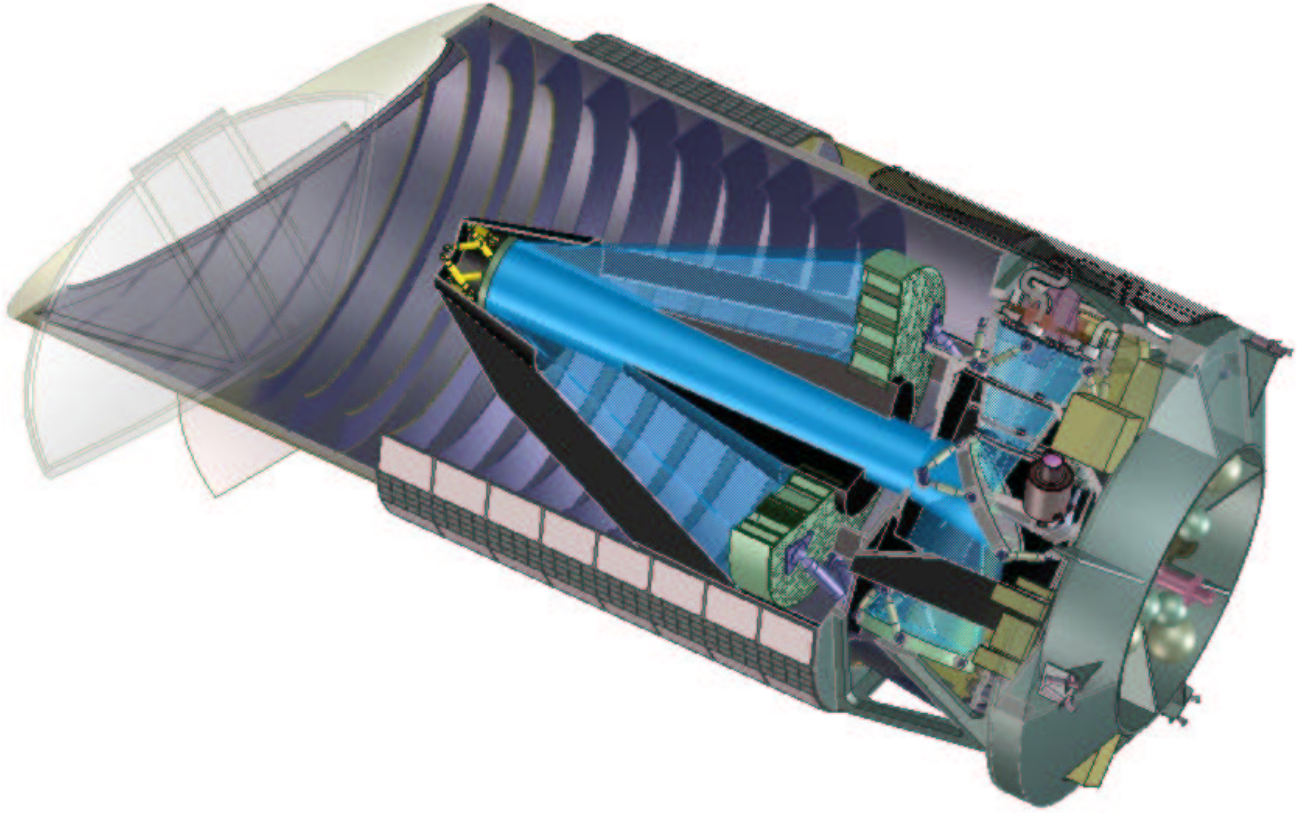


**Figure 3.** A cross-sectional view of the SNAP satellite. The principal assembly components are the telescope, optical bench, instruments, propulsion deck, bus, and thermal shielding.

The intrinsic peak-brightness dispersion of SNe Ia after light-curve shape and extinction correction is  $\sim 10\%$ . In practice, the observed brightness dispersion can increase as much as  $\sim 15\%$  at the highest redshifts due to gravitational lensing, depending on the exact nature of the lenses. So statistically, there is no need to measure the corrected peak brightness to better than  $\sim 10\%$ . Given the limitation of  $\sim 2\%$  systematic errors, we should observe at least  $(0.15/0.02)^2 \approx 50$  supernovae for each redshift bin of interest. We consider this number to be a lower bound; due to the value of using supernova subsets in performing systematic checks (e.g. comparing sets of like supernovae, bootstrap analysis, use of independent calibrators) an even larger data sample would be extremely valuable.

The importance of using supernovae over the full redshift range out to  $z \sim 1.7$  for measuring the cosmological parameters is demonstrated in Fig. 4 which shows the statistical uncertainty in the cosmological parameters  $\Omega_M$ ,  $\Omega_\Lambda$ ,  $\Omega_k$ , and the equation of state ratio of the dark energy,  $w$ , as a function of maximum redshift probed. We assumed 2366 supernovae in the range  $0 \leq z \leq z_{\max}$  with a distribution scaled from the  $z_{\max} = 1.7$  distribution. Each supernova is given an individual statistical uncertainty of 15% arising from an intrinsic dispersion of 0.1 and an observed stretch and color corrected peak brightness uncertainty of 10%. From this figure we conclude the following: 1) using SNe Ia that extend to redshifts of  $z = 1$  and higher helps in obtaining higher accuracy because one covers a larger interval of “action” of the dark energy, and 2) going to redshifts much higher than  $z \approx 2$  is not useful because dark energy’s contribution to the energy-density is negligible for  $z \gtrsim 2$ . However, the SNe beyond  $z > 1$  are extremely valuable for testing models of SN evolution and grey dust, especially with simultaneous NIR measurements.

Although current data indicate that an accelerating dark energy density—perhaps the cosmological constant—has overtaken the decelerating mass density, they do not tell us the actual magnitude of either one. These two density values

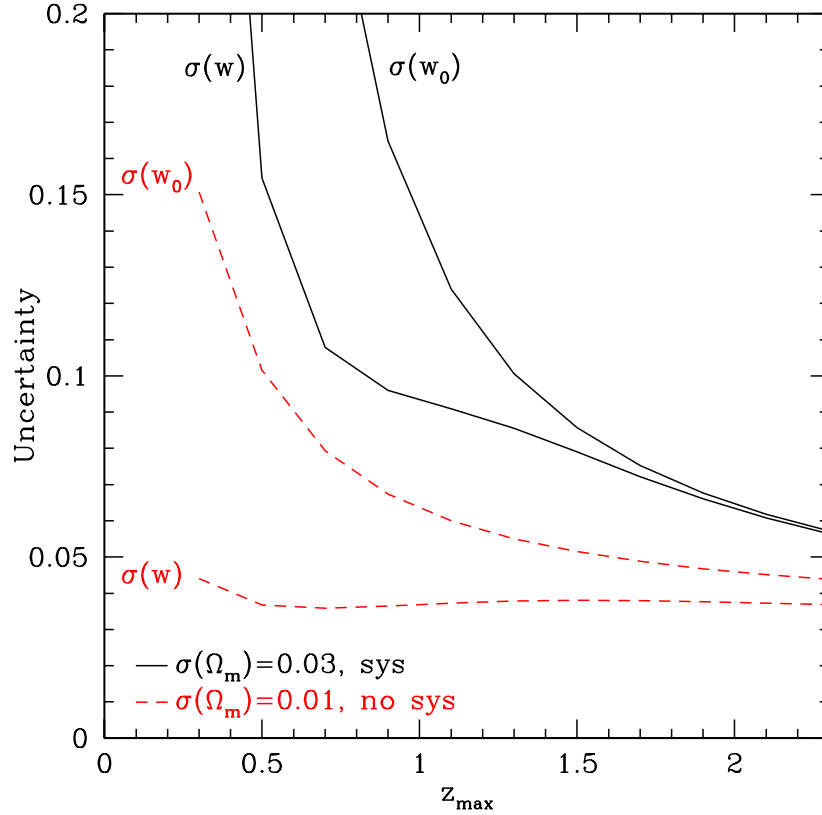


**Figure 4.** Accuracy in parameter estimation as a function of maximum redshift probed in SN Ia surveys. Shown is the statistical uncertainty in the determination of the cosmological parameters  $\Omega_M$ ,  $\Omega_\Lambda$ , and  $\Omega_k$  (upper panel; knowledge of  $w$  assumed) and equation of state ratio  $w$  (lower panel; flat Universe assumed) each as a function of maximum redshift probed  $z_{\text{max}}$ . Approximately 2400 supernovae distributed from  $z = 0$  to  $z_{\text{max}}$  are assumed in each case with statistical uncertainties only. Exploring redshifts between 0 and 1.7 is optimal, since this is where most of the dark energy action occurs. Going to redshifts beyond  $z \sim 1.8$  would bring very little improvement in parameter-determination accuracy, as the dark energy is expected to be dynamically unimportant at such high redshifts.

**Table 1.** SNAP 1- $\sigma$  statistical and systematic uncertainties in parameter determination

	$\sigma_{\Omega_M}$		$\sigma_{\Omega_\Lambda}$ (or $\sigma_{\Omega_{D.E.}}$ )		$\sigma_w$		$\sigma_{w'}$	
	stat	sys	stat	sys	stat	sys	stat	sys
$w = -1$	0.02	0.02	0.05	< 0.01	—	—	—	—
$w = -1$ , flat	—	—	0.01	0.02	—	—	—	—
$w = \text{const}$ , flat	—	—	0.02	0.02	0.05	< 0.01	—	—
$\Omega_M, \Omega_k$ known; $w = \text{const}$	—	—	—	—	0.02	< 0.01	—	—
$\Omega_M, \Omega_k$ known; $w(z) = w + w' z$	—	—	—	—	0.08	< 0.01	0.12	0.15

are two of the fundamental parameters that describe the constituents of our Universe, and determine its geometry and destiny. The proposed satellite project is designed to obtain sufficient brightness-redshift data for a large enough range of redshifts ( $0.1 < z < 1.7$ ) that these absolute densities can each be determined to unprecedented accuracy (see Fig. 1). Taken together, the sum of these energy densities then provides a measurement of the curvature of the Universe. Assuming that the dark energy is the cosmological constant, this experiment can simultaneously determine mass density  $\Omega_M$  to accuracy of 0.02, cosmological constant energy density  $\Omega_\Lambda$  to 0.05 and curvature  $\Omega_k = 1 - \Omega_M - \Omega_\Lambda$  to 0.06. The expected parameter measurement precisions for this and other cosmological scenarios are summarized in Table 1.

The proposed experiment is one of very few that can study the dark energy directly, and test a cosmological constant against alternative dark energy candidates. Assuming a flat Universe with mass density  $\Omega_M$  and a dark energy component with a non-evolving equation of state, the proposed experiment will be able to measure the equation of state ratio  $w$  with accuracy of 0.05 (for constant  $w$ ), at least a factor of five better than the best planned cosmological probes, including systematic errors.<sup>18,19</sup> With such a strong constraint on  $w$  we will be able to differentiate between the cosmological constant and such theoretical alternatives as topological defect models and a range of dynamical scalar-field (“quintessence”) particle-physics models (see Fig. 2). Moreover, with data of such high quality one can relax the assumption of the constant equation of state, and test its variation with redshift, as predicted by many theories including supergravity and M-theory inspired models. These determinations would directly shed light on high energy field theory and physics of the early Universe.

It is important to note that other cosmological measurements are and will be available, providing complementarity and cross comparison. The simultaneous fit can improve constraints by as much as an order of magnitude – or they may not agree and upset our cosmological understanding.

To accomplish a rigorous test discovery and study of more supernovae and more distant supernovae (or any probe) is insufficient. We must address each of the systematic concerns, requiring a major leap forward in the measurement techniques. The science goals have thus driven us to the satellite experiment that we describe in the next section.

## 4. PROPOSED EXPERIMENT

### 4.1. Instrumentation

The baseline proposed satellite experiment is composed of a simple, dedicated combination of a 2.0-meter telescope three-mirror-anastigmat, a 1-square-degree optical – NIR imager and a low resolution ( $R \sim 75$ ) spectrograph sensitive in the wavelength range 3500 – 17000 Å. The mirror aperture is about as small as it can be before photometry and spectroscopy at the requisite resolution is no longer zodiacal-light-noise limited. A smaller mirror design would quickly degrade the achievable signal-to-noise of the spectroscopy measurements, and drastically reduce the number of supernovae followed. The 1-square-degree wide field is obtained with a three-mirror telescope and a feedback loop based on fast-readout chips on the focal plane to stabilize the image. The field of view for the imager has been optimized to obtain the follow-up photometry of multiple supernovae simultaneously; a smaller field would require multiple pointings of the telescope and again would greatly reduce the number of supernovae that could be followed. The spectrograph covers the wavelength range necessary to capture, over the entire target redshift range, the Si II 6150 Å feature that both identifies SNe Ia and provides a key measurement of the explosion physics to probe the progenitor state.

Our baseline configuration (Fig. 5) is a three-mirror anastigmat in which the tertiary mirror re-images an intermediate Cassegrain focus onto the detector plane. This configuration has been analyzed by Ref. 20, 21, and is the fifth design

presented by Ref. 22. This optical train achieves a large flat focal surface with acceptable image quality without the use of refractive correctors. As with other anastigmats, it is free from spherical aberration, coma and astigmatism. There are further practical advantages to this configuration: baffling against stray light is simpler and the focal plane is more accessible. It possesses two beam waists: one at the Cassegrain focus near the primary mirror, and a second midway between the tertiary mirror and the detector plane. This second waist is small, and is an effective location for our CCD shutter. This optic delivers a root-mean-square image blur of 3 microns (0.03'') over a working field of view extending out to 42' off the geometrical axis.

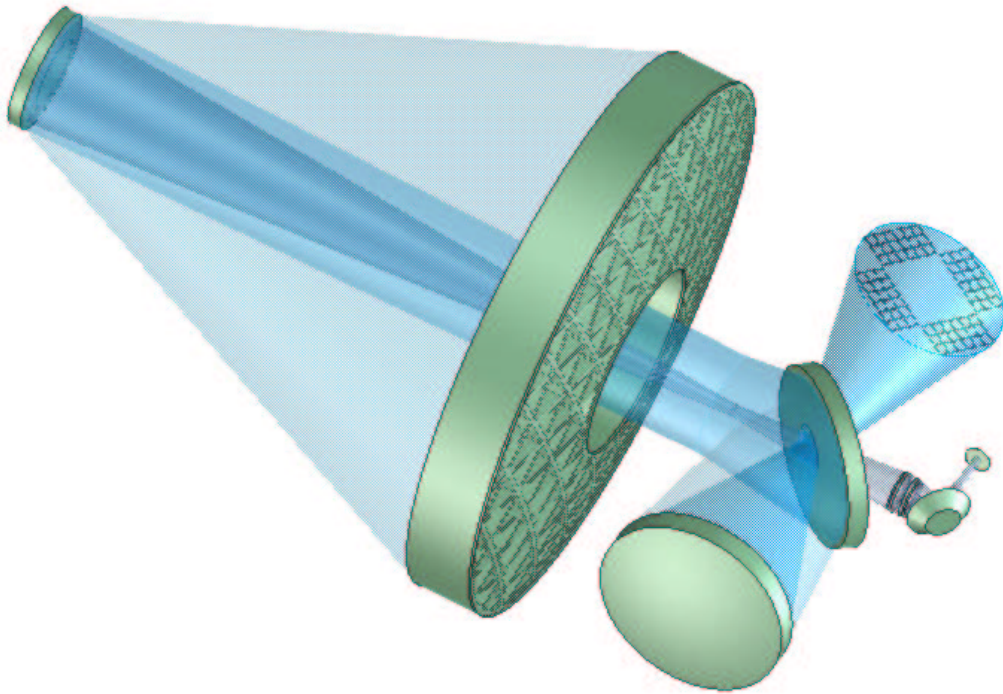


**Figure 5.** Side view of our baseline optical configuration, with a 2.0 meter primary mirror, a 0.45 meter secondary mirror, a folding flat, and a 0.7 meter tertiary mirror.

The wide fields of view of the imagers allow simultaneous batch discovery and photometry of  $\sim 2500$  SNe/year with the proposed accuracy. (The field of view is slightly overscoped due to the large uncertainty in high-redshift supernova rates.) Even higher numbers of more distant, less precisely measured supernovae will be available in our data set. The wide-field imager covers three-quarters of an annular 1 square degree patch of sky with a mosaic of new technology n-type high-resistivity CCD's<sup>23-25</sup> that have high quantum efficiency for wavelengths between 0.3 and 1.0 microns. Each of the  $3k \times 3k$  CCD's have  $10.5 \mu\text{m}$  pixels which give  $0.1''$  per pixel with readout noise of  $4e^-$  and dark current of  $0.08 e^- \text{min}^{-1} \text{pixel}^{-1}$ . The remaining quarter of the annulus is covered by an array of 25 HgCdTe detectors; we will use commercially available  $2k \times 2k$ ,  $1.7 \mu\text{m}$  cutoff devices with  $18 \mu\text{m}$  pixels, high ( $\sim 80\%$ ) quantum efficiency, low ( $\sim 2 e^- \text{min}^{-1} \text{pixel}^{-1}$ ) dark current, and  $4 e^-$  readout noise.<sup>26</sup>

Fixed filters are placed on each detector, arranged in the focal plane such that each piece of sky will be observed in each filter with a shift and stare mode of operation (Figure 6). The relative areas of each filter are proportional to the exposure times needed for the supernova observations. The imager will run a concurrent search and follow-up of

supernovae over the entire redshift range  $0.1 \leq z \leq 1.7$  in wavelengths between 0.35 and 1.7 microns.

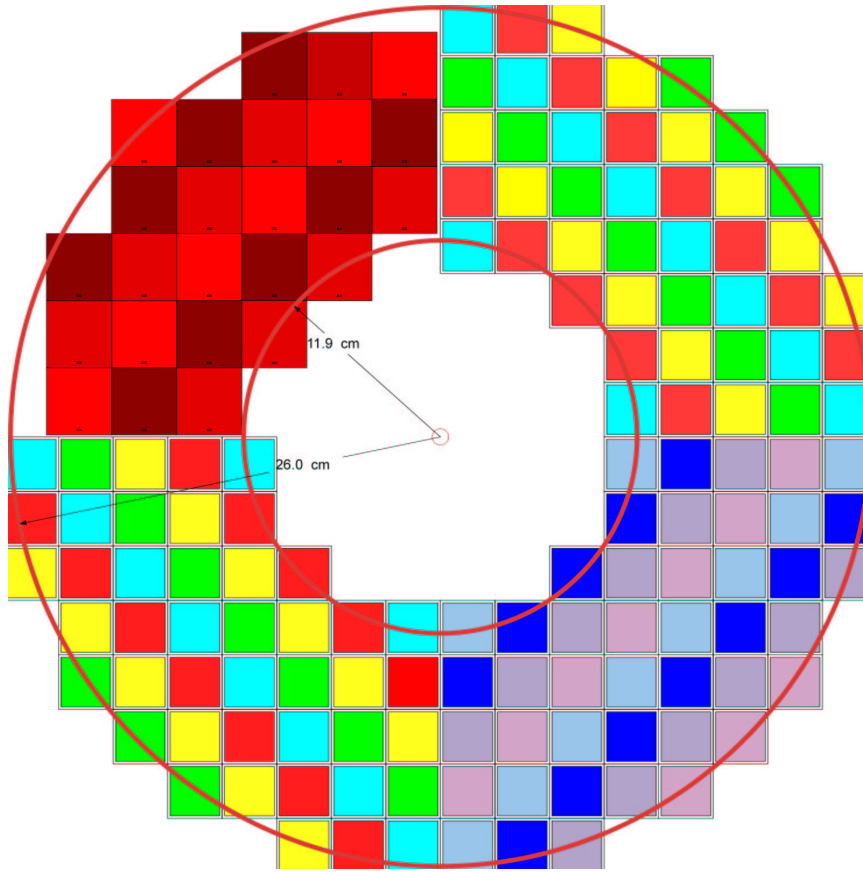


**Figure 6.** The CCD mosaic camera is tiled with 132  $3k \times 3k$  high-resistivity CCD's and 25 HgCdTe detectors and covers one square degree. The annular shape is necessary in a simple three-mirror anastigmat telescope design.

The spectrograph relies on an “integral field unit” (IFU) to obtain an effective image of a  $2'' \times 2''$  field, split into approximately  $0.1''$  by  $2''$  regions that are each individually dispersed to obtain a flux at each position and wavelength (sometimes called a three-dimensional “data cube”). A prism provides a high-throughput dispersive element that makes possible observations of  $z = 1.7$  supernovae with brightness 23.86 magnitudes at  $\lambda = 1.6 \mu\text{m}$  (on the Vega system), with a 2-m aperture telescope. The broad supernova features accommodate the low dispersion and the decreasing resolution for increasing wavelengths naturally follows the feature broadening at higher redshifts. The detector is a single thinned HgCdTe chip (whose technology is in development for the NGST) that will provide high quantum efficiency from  $0.4 - 1.7 \mu\text{m}$ . In operation, the integral field unit will allow simultaneous spectroscopy of a supernova target and its surrounding galactic environment; the  $2''$  by  $2''$  field of view also removes any requirement for precise positioning of a supernova target in a traditional spectrograph slit and simplifies eventual reference galaxy subtraction. This point is particularly important for absolute flux calibration, because all of the supernova light is collected with the integral field units. The spectrograph is thus designed to allow use of the spectra to obtain photometry in any “synthetic” filter band that one chooses.

## 4.2. Observation Strategy and Baseline Data Package

This instrumentation will be used with a simple, predetermined observing strategy designed to repeatedly monitor a 20-square-degree region of sky near the north and south ecliptic poles, discovering and following supernovae that explode in that region. Every field will be visited frequently enough with sufficiently long exposures that at any given redshift up to  $z = 1.5$  every supernova will be discovered within, on average, two restframe days of explosion. (Supernovae at much

higher redshifts will be found slightly later in their light curve rise times.) The periodic observation of fixed fields ensures that every supernova at  $z < 1.7$  will be followed as it brightens and fades.

The wide-field imager makes it possible to find and follow with precision photometry and spectroscopy approximately 2500 SNe Ia in a year. The 2.0-meter aperture of the mirror, along with high throughput NIR instruments, allow this dataset to extend to redshift  $z = 1.7$ .

This prearranged observing program will provide a uniform, standardized, calibrated dataset for each supernova, allowing for the first time comprehensive comparisons across complete sets of supernovae. The standardized dataset will comprise the following strategies and measurements that will address, and often eliminate, the statistical and systematic uncertainties described in § 2.

- Blind searching.
- Batch processing (unbiased searching).
- SNe Ia at  $0.1 \leq z \leq 1.7$ .
- $\sim 75$  SNe Ia per 0.03 redshift bin.
- Spectrum for every supernova at maximum covering the rest frame Si II 6250Å feature.
- Spectral time series of representative SN Ia with cross-wavelength relative flux calibration.
- A light curve sampled at frequent, standardized intervals that extends from  $\sim 2$ -80 restframe days after explosion to obtain a stretch and extinction-corrected peak rest-frame  $B$  brightness to 10% (same order as the Type Ia intrinsic dispersion).
- Multiple color measurements in up to 12 bands, including rest-frame  $B$  and  $V$  bands, at key epochs on the light curve.
- Final reference images and spectra to enable clean subtraction of host galaxy light.

The quality of these measurements is as important as the time and wavelength coverage, so we require:

- Control over signal-to-noise ratio for these photometry and spectroscopy measurements, to permit comparably high statistical significance for supernovae over a wide range of redshifts.
- Control over calibration for these photometry and spectroscopy measurements, with constant monitoring data collected to ensure that cross-instrument and cross-wavelength calibration remain stable over time.

Note that to date no single SN Ia has ever been observed with this complete set of measurements, either from the ground or in space, and only a handful have a dataset that is comparably thorough. With the observing strategy proposed here, *every one* of  $\sim 2000$  followed SN Ia will have this complete set of measurements.

The satellite instrumentation and observation strategy is designed to provide the precision cosmological measurements summarized in Table 1 with comprehensive control of statistical and previously identified or proposed sources of systematic uncertainty. Simulations show that systematic errors must be lower than  $\sim 2\%$  in order to achieve these science goals. In turn, photometric measurements of each point on the light curve are tuned so that shape and extinction corrected peak brightnesses of individual supernovae are known to  $\sim 10\%$ , the same order of magnitude as their intrinsic dispersion. Large numbers ( $\sim 75$ ) of supernova in each redshift bin then reduce the statistical uncertainties toward the systematic limit.

Each systematic will either be measured, so that it can become part of the statistical error budget, or bounded. In addition the completeness of the dataset will make it possible to monitor the physical properties of each supernova explosion, allowing studies of effects that have not been previously identified or proposed.

## 5. CONCLUSION

The surprising discoveries of recent years make this a fascinating new era of empirical cosmology, addressing fundamental questions. This proposed satellite project presents a unique opportunity to extend this exciting work and advance our understanding of the Universe. The origin and destiny of the Universe are extraordinary, intriguing questions; we live at a time when we can begin to find answers.

## ACKNOWLEDGMENTS

This work was supported by the U.S. Department of Energy under contract No. DE-AC03-76SF00098.

## REFERENCES

1. Perlmutter, S. and Aldering, G. and Goldhaber, G. and Knop, R. A. and Nugent, P. and Castro, P. G. and Deustua, S. and Fabbro, S. and Goobar, A. and Groom, D. E. and Hook, I. M. and Kim, A. G. and Kim, M. Y. and Lee, J. C. and Nunes, N. J. and Pain, R. and Pennypacker, C. R. and Quimby, R. and Lidman, C. and Ellis, R. S. and Irwin, M. and McMahon, R. G. and Ruiz-Lapuente, P. and Walton, N. and Schaefer, B. and Boyle, B. J. and Filippenko, A. V. and Matheson, T. and Fruchter, A. S. and Panagia, N. and Newberg, H. J. M. and Couch, W. J. and The Supernova Cosmology Project, "Measurements of Omega and Lambda from 42 High-Redshift Supernovae," *Astrophys J.* **517**, pp. 565–586, 1999.
2. A. G. Riess, A. V. Filippenko, P. Challis, A. Clocchiatti, A. Diercks, P. M. Garnavich, R. L. Gilliland, C. J. Hogan, S. Jha, R. P. Kirshner, B. Leibundgut, M. M. Phillips, D. Reiss, B. P. Schmidt, R. A. Schommer, R. C. Smith, J. Spyromilio, C. Stubbs, N. B. Suntzeff, and J. Tonry, "Observational Evidence from Supernovae for an Accelerating Universe and a Cosmological Constant," *Astron. J.* **116**, pp. 1009–1038, 1998.
3. N. A. Bahcall, J. P. Ostriker, S. Perlmutter, and P. J. Steinhardt, "The Cosmic Triangle: Revealing the State of the Universe," *Science* **284**, pp. 1481–+, 1999.
4. A. Balbi, P. Ade, J. Bock, J. Borrill, A. Boscaleri, P. De Bernardis, P. G. Ferreira, S. Hanany, V. Hristov, A. H. Jaffe, A. T. Lee, S. Oh, E. Pascale, B. Rabii, P. L. Richards, G. F. Smoot, R. Stompor, C. D. Winant, and J. H. P. Wu, "Constraints on Cosmological Parameters from MAXIMA-1," *Astrophys. J.* **545**, pp. L1–LL4, 2000.
5. A. E. Lange, P. A. Ade, J. J. Bock, J. R. Bond, J. Borrill, A. Boscaleri, K. Coble, B. P. Crill, P. de Bernardis, P. Farese, P. Ferreira, K. Ganga, M. Giacometti, E. Hivon, V. V. Hristov, A. Iacoangeli, A. H. Jaffe, L. Martinis, S. Masi, P. D. Mauskopf, A. Melchiorri, T. Montroy, C. B. Netterfield, E. Pascale, F. Piacentini, D. Pogosyan, S. Prunet, S. Rao, G. Romeo, J. E. Ruhl, F. Scaramuzzi, and D. Sforna, "Cosmological parameters from the first results of Boomerang," *Phys. Rev. D* **63**, pp. 42001–+, 2001.
6. R. R. Caldwell, R. Dave, and P. J. Steinhardt, "Cosmological Imprint of an Energy Component with General Equation of State," *Physical Review Letters* **80**, pp. 1582–1585, 1998.
7. I. Zlatev, L. Wang, and P. J. Steinhardt, "Quintessence, Cosmic Coincidence, and the Cosmological Constant," *Physical Review Letters* **82**, pp. 896–899, 1999.
8. J. A. Frieman, C. T. Hill, A. Stebbins, and I. Waga, "Cosmology with Ultralight Pseudo Nambu-Goldstone Bosons," *Physical Review Letters* **75**, pp. 2077–2080, 1995.
9. K. Coble, S. Dodelson, and J. A. Frieman, "Dynamical  $\Lambda$  models of structure formation," *Phys. Rev. D* **55**, pp. 1851–1859, 1997.
10. A. Vilenkin, "String-Dominated Universe," *Physical Review Letters* **53**, pp. 1016–1018, 1984.
11. A. Vilenkin and E. Shellard, *Cosmic Strings and other Topological Defects*, Cambridge University Press, Cambridge, U.K., 1994.
12. P. M. Garnavich, S. Jha, P. Challis, A. Clocchiatti, A. Diercks, A. V. Filippenko, R. L. Gilliland, C. J. Hogan, R. P. Kirshner, B. Leibundgut, M. M. Phillips, D. Reiss, A. G. Riess, B. P. Schmidt, R. A. Schommer, R. C. Smith, J. Spyromilio, C. Stubbs, N. B. Suntzeff, J. Tonry, and S. M. Carroll, "Supernova Limits on the Cosmic Equation of State," *Astrophys. J.* **509**, pp. 74–79, 1998.
13. M. Hamuy, M. M. Phillips, N. B. Suntzeff, R. A. Schommer, J. Maza, and R. Aviles, "The Absolute Luminosities of the Calan/Tololo Type IA Supernovae," *Astron. J.* **112**, pp. 2391–+, 1996.
14. M. Hamuy, S. C. Trager, P. A. Pinto, M. M. Phillips, R. A. Schommer, V. Ivanov, and N. B. Suntzeff, "A Search for Environmental Effects on Type IA Supernovae," *Astron. J.* **120**, pp. 1479–1486, 2000.

15. P. Hoefflich, J. C. Wheeler, and F. K. Thielemann, "Type IA Supernovae: Influence of the Initial Composition on the Nu cleosynthesis, Light Curves, and Spectra and Consequences for the Determination of Omega M and Lambda," *Astrophys. J.* **495**, pp. 617–+, 1998.
16. E. J. Lentz, E. Baron, D. Branch, P. H. Hauschildt, and P. E. Nugent, "Metallicity Effects in Non-LTE Model Atmospheres of Type IA Supernovae," *Astrophys. J.* **530**, pp. 966–976, 2000.
17. P. Nugent, M. Phillips, E. Baron, D. Branch, and P. Hauschildt, "Evidence for a Spectroscopic Sequence among Type Ia Supernovae," *Astrophys. J.* **455**, pp. L147–+, 1995.
18. J. Weller and A. Albrecht, "Opportunities for Future Supernova Studies of Cosmic Acceleration," *Physical Review Letters* **86**, pp. 1939–1942, 2001.
19. J. Weller and A. Albrecht, "Future supernovae observations as a probe of dark energy," *Phys. Rev. D* **65**, p. TBD, 2002.
20. L. G. Cook, "Three-mirror anastigmat used off-axis in aperture and field," in *Space optics; Proceedings of the Seminar, Huntsville, Ala., May 22-24, 1979. (A80-17432 05-89) Bellingham, Wash., Society of Photo-Optical Instrumentation Engineers, 1979, p. 207-211.*, **183**, pp. 207–211, 1979.
21. S. G. L. Williams, "On-axis three-mirror anastigmat with an offset field of view," in *Space optics; Proceedings of the Seminar, Huntsville, Ala., May 22-24, 1979. (A80-17432 05-89) Bellingham, Wash., Society of Photo-Optical Instrumentation Engineers, 1979, p. 212-217.*, **183**, pp. 212–217, 1979.
22. D. Korsch, "Design and optimization technique for three-mirror telescopes," *Applied Optics* **19**, pp. 3640–3645, 1980.
23. S. E. Holland, M. Wei, K. Ji, W. E. Brown, D. K. Gilmore, R. J. Stover, D. E. Groom, M. E. Levi, N. Palaio, and S. Perlmutter, "Large Format CCD Image Sensors Fabricated on High Resistivity Silicon," in *IEEE Workshop on Charge-Coupled Devices and Advanced Image Sensors*, pp. 239–+, 1999.
24. R. J. Stover, M. Wei, K. Ji, W. E. Brown, D. K. Gilmore, S. E. Holland, D. E. Groom, M. E. Levi, N. Palaio, and S. Perlmutter, "A 2Kx2K high resistivity CCD," in *Optical Detectors for Astronomy II: State-of-the-Art at the Turn of the Millenium*, pp. 239–+, 2000.
25. D. E. Groom, S. E. Holland, M. E. Levi, N. P. Palaio, S. Perlmutter, R. J. Stover, and M. Wei, "Back-illuminated, fully-depleted CCD image sensors for use in optical and near-IR astronomy," *Nuclear Instruments and Methods in Physics Research A* **442**, pp. 216–222, 2000.
26. J. Johnson, E. Polidan, A. Waczynski, R. Hill, G. Delo, M. Robberto, C. M. Lisse, and L. Cawley, "Dark current measurements on a state of the art near-IR HgCdTe 1024×1024 array,"